Redox Biology 34 (2020) 101587

Contents lists available at ScienceDirect

Redox Biology

journal homepage: www.elsevier.com/locate/redox

Peroxynitrite promotes serine-62 phosphorylation-dependent stabilization of the oncoprotein c-Myc

Deepika Raman[a], Stephen J.F. Chong[a,b], Kartini Iskandar[a], Jayshree L. Hirpara[c], Shazib Pervaiz[a,d,e,*]

[a] Department of Physiology, Yong Loo Lin School of Medicine, National University of Singapore (NUS), Singapore
[b] Department of Medical Oncology, Dana-Farber Cancer Institute, Boston, MA, USA
[c] Cancer Science Institute of Singapore, National University of Singapore, Singapore
[d] NUS Graduate School for Integrative Sciences and Engineering, National University of Singapore, Singapore
[e] National Cancer Institute of Singapore, National University Health System, Singapore

A B S T R A C T

Stabilization of c-Myc oncoprotein is dependent on post-translational modifications, especially its phosphorylation at serine-62 (S62), which enhances its tumorigenic potential. Herein we report that increase in intracellular superoxide induces phospho-stabilization and activation of c-Myc in cancer cells. Importantly, sustained phospho-S62 c-Myc was necessary for promoting superoxide dependent chemoresistance as non-phosphorylatable S62A c-Myc was insensitive to the redox impact when subjected to chemotherapeutic insults. This redox-dependent sustained S62 phosphorylation occurs through nitrative inhibition of phosphatase, PP2A, brought about by peroxynitrite, a reaction product of superoxide and nitric oxide. We identified a conserved tyrosine residue (Y238) in the c-Myc targeting subunit B56α of PP2A, which is selectively amenable to nitrative inhibition, further preventing holoenzyme assembly. In summary, we have established a novel mechanism wherein the pro-oxidant microenvironment stimulates a pro-survival milieu and reinforces tumor maintenance as a functional consequence of c-Myc activation through its sustained S62 phosphorylation via inhibition of phosphatase PP2A.

Significance statement: Increased peroxynitrite signaling in tumors causes sustained S62 c-Myc phosphorylation by PP2A inhibition. This is critical to promoting c-Myc stabilization and activation which promotes chemoresistance and provides significant proliferative and growth advantages to osteosarcomas.

1. Introduction

Cancer cells have a distinct redox milieu that serves as a terrain for pleiotropic signaling impinging on cell fate decisions. The pro-oncogenic ROS milieu serves as a hotbed of deregulated pathways that may occur through either activation of oncogenes or the loss-of-function of tumor suppressor proteins. While several theories have been touted, no singular theory has completely satisfied the dynamic nature of the pro-oncogenic trajectory attributed to this cellular redox switch. To that end, it has been demonstrated that a mild increase in intracellular superoxide ($O_2^{\bullet-}$) levels can either promote signal transduction favoring cell proliferation or buffer cancer cells from apoptotic stimuli, thereby promoting chemoresistance [1–7]. In an attempt to decipher the cellular targets and molecular mechanisms underlying the pro-survival activity of a mild pro-oxidant milieu, our recent work provides evidence to implicate $O_2^{\bullet-}$ and/or peroxynitrite ($ONOO^-$; generated from the reaction between $O_2^{\bullet-}$ and nitric oxide) in the pro-oncogenic activities of Bcl-2 and Rac-1 [8–13].

Notably, c-Myc is a master regulator of cell survival and proliferation genes, and its deregulation is associated with a host of human malignancies. c-Myc is activated through a signaling cascade initiated by receptor tyrosine kinase-mediated RAS activation [14]. During homeostasis, the pro-survival activities regulated by c-Myc are counter-balanced through its rapid turnover by way of regulatory constraints. The impaired balance between mitogenic signaling and the proteasomal machinery leads to deregulated c-Myc signaling and activation of its cellular targets that endows cancer cells with a survival advantage [15–19]. Mitogenic signaling controls the phosphorylation of c-Myc at the N-terminal transactivation domain wherein ERK phosphorylates c-Myc at S62 and leads to its stabilization, while GSK-3β mediates the destabilizing c-Myc phosphorylation at the threonine-58 residue. Dually phosphorylated c-Myc is recognised as a substrate by the phosphatase PP2A, which proceeds to dephosphorylate c-Myc at the S62 site, subsequently priming singly phosphorylated c-Myc for degradation by the 26S proteasome [14,20].

Here we report that pharmacological or genetic approaches to tailor tumor redox milieu to promote cell survival and/or inhibition of drug-induced apoptosis is associated with significant enhanced stability and

* Corresponding author. Department of Physiology and Medical Science Cluster Cancer Program, Yong Loo Lin School of Medicine, National University of Singapore, 2 Medical Drive, Building MD9, Singapore, 117593, Singapore.
E-mail addresses: phssp@nus.edu.sg, shazib_pervaiz@nuhs.edu.sg (S. Pervaiz).

https://doi.org/10.1016/j.redox.2020.101587
Received 25 February 2020; Received in revised form 22 April 2020; Accepted 14 May 2020
Available online 16 May 2020

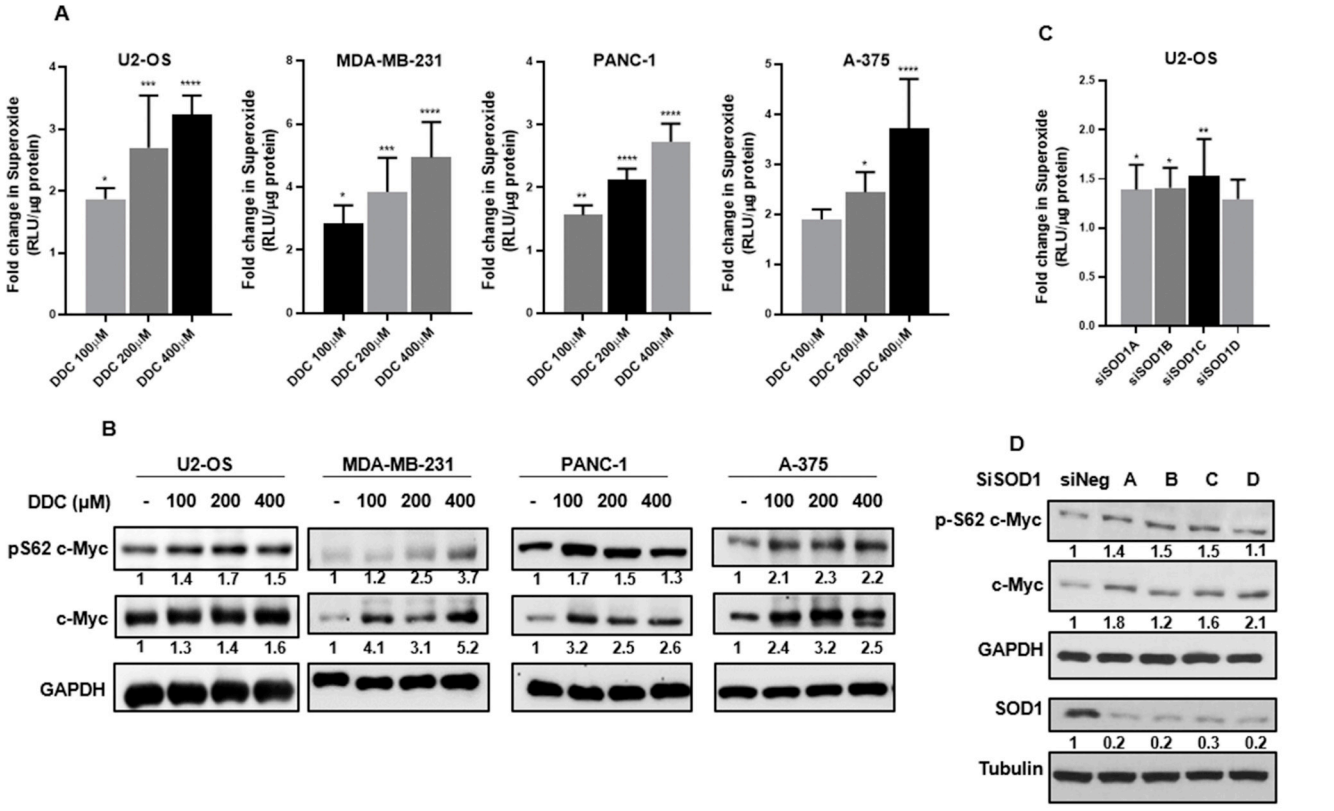

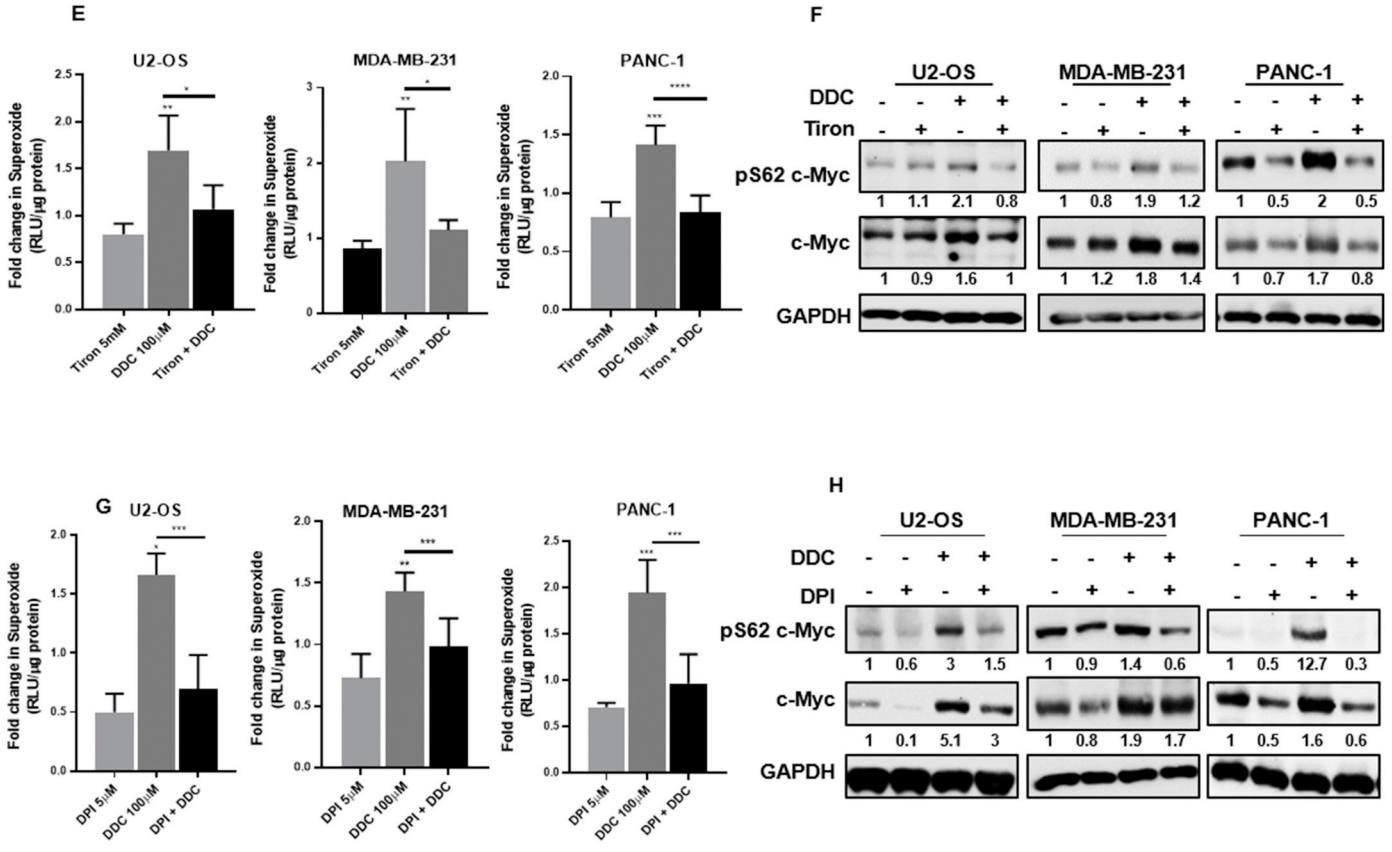

(caption on next page)

Fig. 1. ***c-Myc phosphorylation and stabilization are modulated by intracellular superoxide concentrations***. (A) Modulation in intracellular superoxide concentrations in cell lines challenged with DDC was determined by the Lucigenin chemiluminescence assay. Fold change in superoxide is normalized to control. (B) Representative western blots depicting S62 phosphorylation of c-Myc and stabilization of c-Myc protein in the presence of DDC in the respective cell lines. (C) Lucigenin chemiluminescence assay to determine changes in intracellular superoxide levels in U2-OS cells when challenged with 100 nM siRNA directed against SOD1. Fold change in superoxide is normalized to siNeg (non-targeting siRNA sequence) (D) Representative Western blot to depict S62 phosphorylation of c-Myc and stabilization of total c-Myc protein upon knock-down of SOD1 (100 nM siRNA). (E and G) Representative cell lines were challenged with Tiron (5 mM) and DPI (5 μM) and the Lucigenin chemiluminescence assay was performed to ascertain the changes in intracellular superoxide concentrations. Fold change in superoxide was normalized to control. DDC concentration was standardized at 100 μM. (F and H) Western blot analysis of pS62 c-Myc and total c-Myc protein in cell lines subjected to Tiron (5 mM) and DPI (5 μM) treatments. Fold change in superoxide was normalized to control. DDC concentration was standardized at 100 μM. One-way ANOVA was employed for statistical analysis (* = $p < 0.05$, ** = $p < 0.01$, *** = $p < 0.001$, **** = $p < 0.0001$).

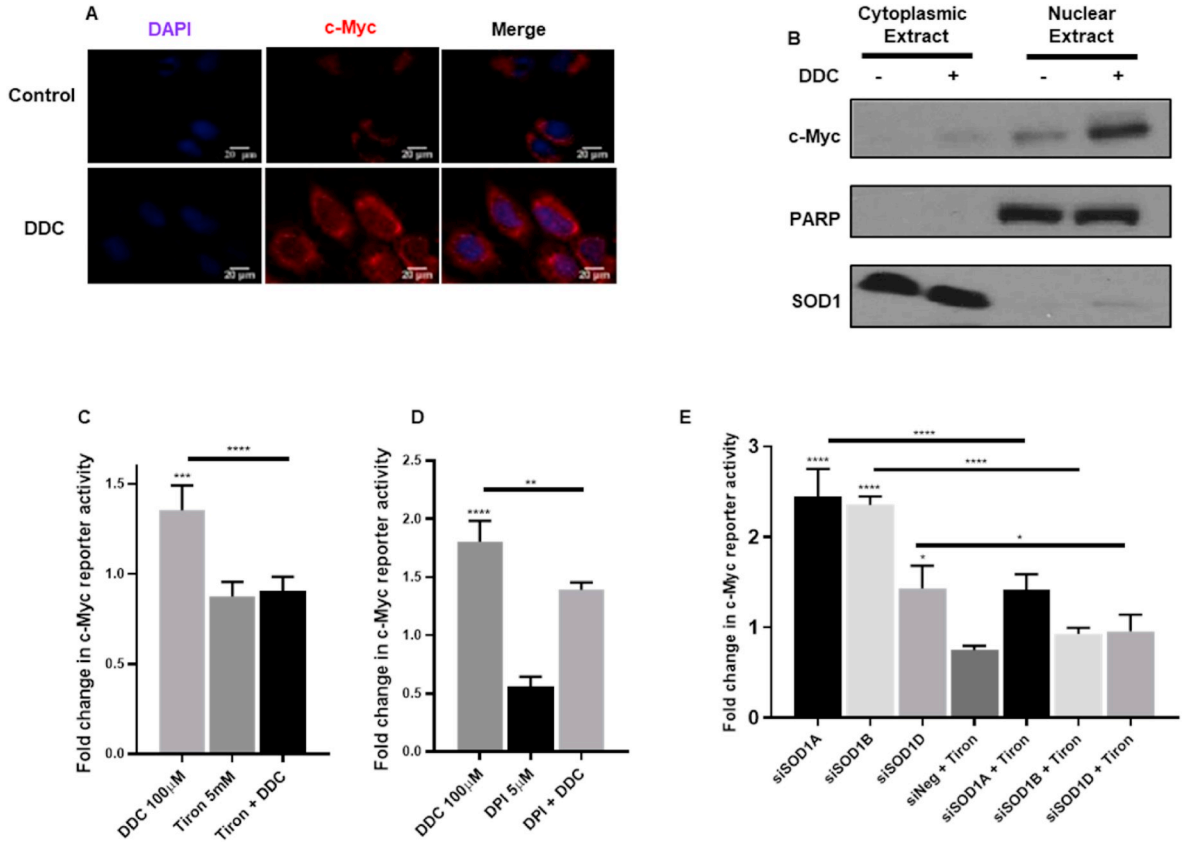

Fig. 2. ***Elevated intracellular superoxide levels correspond with an increased nuclear accumulation of c-Myc as well as its transactivation.*** (A) Representative immunofluorescence images of U2-OS cells indicate colocalization of c-Myc (Red) and nucleus (DAPI) in the presence of DDC (100 μM). (B) Western blot analyses demonstrates increased c-Myc protein accumulation in U2-OS cells in the nuclear fraction in DDC (100 μM) treated cells. Fractions were delineated by use of the nuclear marker PARP and cytoplasmic marker SOD1. (C and D) c-Myc reporter luciferase assay determines modulation of c-Myc transactivation in the presence of DDC (100 μM–4 h), Tiron (5 mM–5 h, 1 h pre-treatment for Tiron + DDC) and DPI (5 μM-18 h, 14 h pre-treatment in case of DPI + DDC) in U2-OS cells. Fold change in c-Myc reporter activity was normalized to vehicle control. (E) c-Myc transactivation luciferase assay analysis to determine c-Myc reporter activity when challenged by siRNA (100 nM) directed against SOD1 alone (24 h) or siSOD1 (19 h) followed by subsequent 5 h treatment with Tiron in U2-OS cells. Fold change in c-Myc luciferase reporter activity was normalized to siNeg. One-way ANOVA was employed for statistical analysis (* = $p < 0.05$, ** = $p < 0.01$, *** = $p < 0.001$, **** = $p < 0.0001$). (For interpretation of the references to colour in this figure legend, the reader is referred to the Web version of this article.)

activity of c-Myc. $O_2^{\bullet-}$ driven $ONOO^-$ mediated stability of c-Myc is a function of its sustained phosphorylation at S62. Notably, our work implicates redox modification of B56α binding subunit of PP2A, responsible for S62 dephosphorylation/inactivation of c-Myc, thereby preventing PP2A holoenzyme assembly and maintaining c-Myc in its active form to promote cell survival. In summary, we have uncovered a novel therapeutic target in PP2A activation, which can be exploited to pull the brakes on a yet non-targetable oncoprotein c-Myc.

2. Results

2.1. Increase in intracellular $O_2^{\bullet-}$ is associated with c-Myc phosphorylation and abundance

To investigate the role of $O_2^{\bullet-}$ in effecting changes on the oncoprotein c-Myc, we made use of DDC, a known pharmacological inhibitor of SOD1. A panel of cell lines derived from solid tumors was chosen wherein c-Myc either drives tumorigenesis or facilitates tumor progression. By blocking the disproportionation of $O_2^{\bullet-}$ to H_2O_2, DDC treatment for 4 h was able to increase the levels of intracellular $O_2^{\bullet-}$ in a dose-dependent manner (Fig. 1A). A concomitant increase in the levels of phospho-S62 c-Myc and total c-Myc protein was observed (Fig. 1B). A time kinetic assay employing a 100 μM DDC dose was

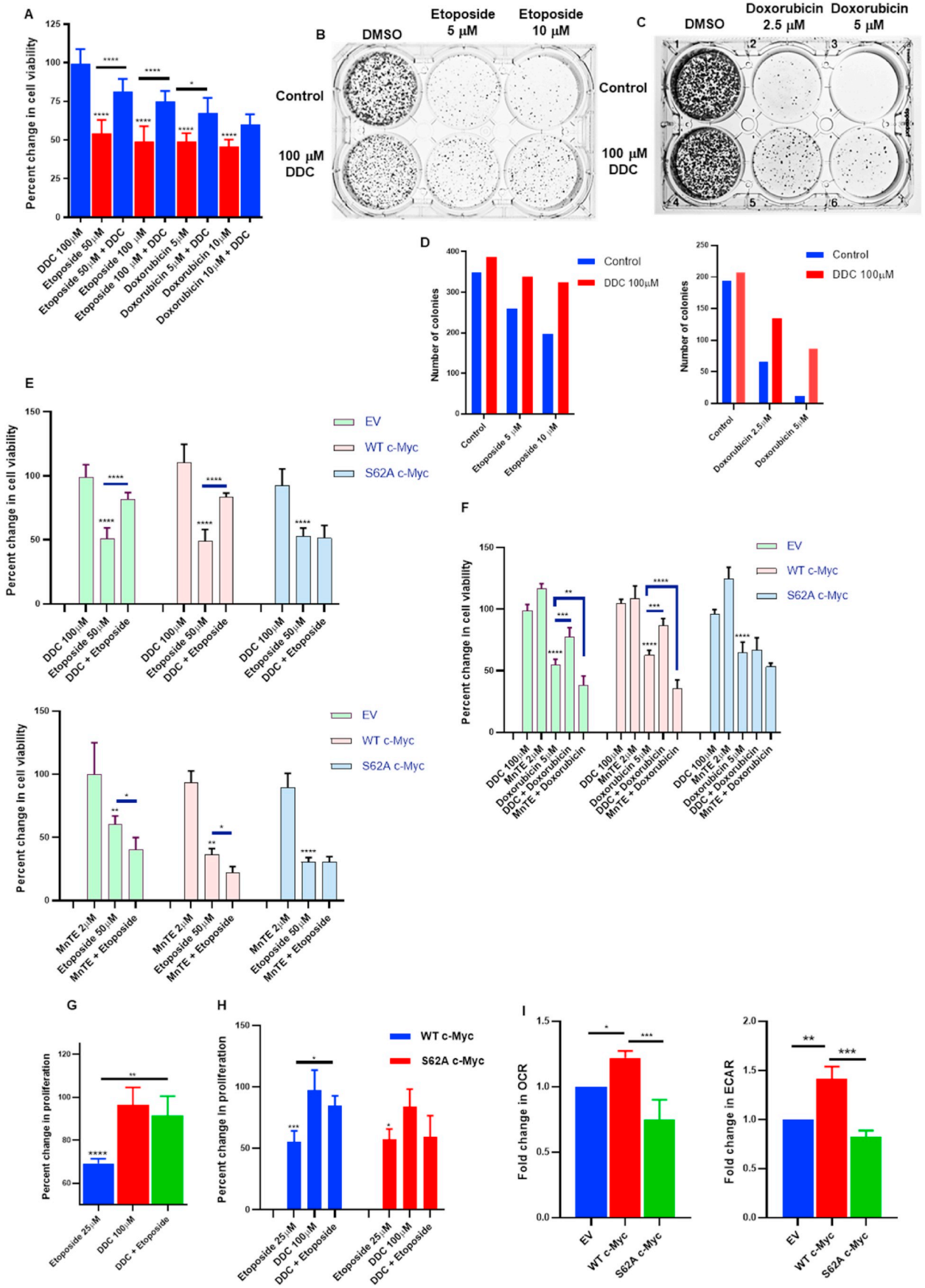

(caption on next page)

Fig. 3. ***Superoxide mediated phospho-serine-62 c-Myc is critical for enhancing the chemoresistance potential of cancer cells as well as making them more energetic***. (A) MTT cell viability assay represents rescue of U2-OS cells from chemotherapy (Etoposide/Doxorubicin 24 h) challenged cell death in the presence of DDC (1 h pretreatment). Percent change in cell viability was normalized against vehicle control. (B and C) Representative clonogenic assay to ascertain colony forming ability in chemotherapy challenged cells in the presence of DDC. (D) Representative colonies in each well (3B and 3C) were determined by the Clono counter software. (E and F) MTT cell viability was performed to assess cell viability of stably transfected c-Myc phospho-mutants when challenged with chemotherapeutic drugs (24 h treatment) in the presence of SOD1 inhibitor DDC (1 h pretreatment) and SOD1 mimetic MnTE (2 h pretreatment). Percent change in cell viability was normalized against respective vehicle control. (G) BrDU cell proliferation assay was performed to assess cell viability of U2-OS cells when challenged with Etoposide (24 h) in the presence of DDC (1 h pretreatment). (H) BrDU cell proliferation assay was performed to assess cell viability of U2-OS stably transfected c-Myc phospho-mutants when challenged with Etoposide (24 h) in the presence of SOD1 inhibitor DDC (1 h pretreatment). Percent change in cell proliferation was normalized to vehicle control for U2-OS and WT c-Myc overexpressing U2-OS cells for comparison of the non-phosphorylatable S62A mutant (I) The respiratory and glycolytic profile of cells was analyzed by the Seahorse live cell XF analyzer. Fold change was normalized to empty vector control. One-way ANOVA was employed for statistical analysis (* = $p < 0.05$, ** = $p < 0.01$, *** = $p < 0.001$, **** = $p < 0.0001$).

performed, which indicated that c-Myc protein levels peaked at 4 h post DDC treatment in U2-OS cells (Fig. S1A). Therefore, a 100 μM DDC dose and 4 h treatment were chosen for subsequent experiments. Notably, c-Myc has two separate phosphorylation sites at threonine-58 (T58) and serine-62 (S62) on its N-terminal transactivation domain that are known to reciprocally regulate its stability. Further investigation confirmed that while c-Myc is reproducibly phosphorylated at the S62 residue when challenged with incremental doses of DDC for 4 h, the phosphorylation at the T58 residue was not regulated by an increase in intracellular $O_2^{\bullet-}$ (Fig. S1B). Antibody specificity for the phospho-residues was confirmed by using the stably transfected different point mutants of c-Myc (Fig. S1C). Furthermore, another pharmacological compound ATN-224, also known to inhibit SOD1 activity, was similarly able to recapitulate the increase in $O_2^{\bullet-}$ as well as the phenotypical upregulation in c-Myc stabilization and phosphorylation in a dose-dependent manner at 6 h (Figs. S1D and S1E). Next, we investigated the effect of knock-down of *SOD1* in the regulation of c-Myc phosphorylation and activity. Corroborating the results obtained with pharmacological inhibitors of SOD1, knock-down of *SOD1* for 24 h resulted in an increase in intracellular $O_2^{\bullet-}$, which was further associated with an increase in c-Myc phospho-stabilization (Fig. 1C and D). Finally, to mitigate the levels of $O_2^{\bullet-}$ in cells, a pharmacological scavenger, Tiron (1 h pre-treatment), and the NADPH oxidase (NOX) inhibitor, DPI, were employed. Exposure of cells to Tiron led to the concurrent ablation of c-Myc phosphorylation and $O_2^{\bullet-}$ levels (Fig. 1E and F). Likewise, pre-incubation of cells with DPI (14 h pre-treatment) led to a drop in intracellular phospho-stabilization of c-Myc, concurrently with a decrease in the intracellular $O_2^{\bullet-}$ levels (Fig. 1G and H).

2.2. Increase in intracellular $O_2^{\bullet-}$ promotes nuclear accumulation and transactivation of c-Myc

c-Myc is reported to influence virtually all promoters in an open chromatin complex as well as enhancers, thereby initiating transcription of downstream genes leading to either activation or repression of genes transcribed by RNA polymerase [21–23]. We therefore sought to determine if $O_2^{\bullet-}$ mediated phosphorylation contributed to the activation of intrinsic transcription factor functions of c-Myc in the cell. The pro-oxidant milieu meted by DDC (4 h) was able to promote the translocation of c-Myc protein to the nucleus (Fig. 2A and B). Furthermore, the c-Myc transactivation assay also surmised that, in the presence of elevated intracellular $O_2^{\bullet-}$, c-Myc reporter activation of its downstream targets was enhanced. Additionally, *a priori* treatment with Tiron (1 h) or DPI (14 h) was successfully able to block or reduce DDC (4 h) mediated upregulation of c-Myc reporter activity, respectively (Fig. 2C and D). Furthermore, treatment of cells transfected with siRNA against *SOD1* with Tiron resulted in rescuing c-Myc activation to near-basal levels (Fig. 2E).

Previous studies have pointed to the correlation between c-Myc expression in cells and increase in glycolytic pathway activation driving the Warburg effect as well as genes controlling cell cycle dynamics and DNA repair and stabilization [24–29]. Serendipitously, c-Myc target gene products regulating these processes are further observed to be regulated in response to pharmacological increase in $O_2^{\bullet-}$ (Figs. S2A and S2B) by DDC (4 h).

To determine if the phenotypic changes on c-Myc phospho-stabilization and activation were specific to changes in intracellular $O_2^{\bullet-}$, experiments employing H_2O_2 as well as the general ROS scavenger N-acetyl cysteine (NAC) treatments were performed and c-Myc activity was ascertained. While H_2O_2 treatment (2 h) indeed led to a steep decline in c-Myc activity, it had little or no effect on c-Myc protein levels (Figs. S2C and S2D). This might indicate the inhibition of c-Myc activation through a separate pathway, wherein c-Myc activation was governed independent of its post-translational phosphorylation at S62 and distinct from the regulatory effects meted by $O_2^{\bullet-}$. On the contrary, while NAC (1 h pre-treatment) alone clearly had no effect on c-Myc reporter activity, it was able to satisfactorily neutralize the increase in c-Myc transactivation in response to DDC treatment (Fig. S2E). This can be likely attributed to the effect of the broad-range antioxidant activity of NAC predisposing it to scavenge ROS generated downstream of $O_2^{\bullet-}$ radical in the cells.

2.3. S62 phosphorylation of c-Myc mediates chemoresistance and is a critical determinant of mitochondrial metabolism

Our previous observations have linked increased intracellular $O_2^{\bullet-}$ to inhibition of apoptosis and cancer cell survival. Therefore, we next asked if the death inhibitory effect of an increase in $O_2^{\bullet-}$ was a function of sustained S62 phosphorylation of c-Myc. Firstly, we show that pre-treatment of cells with DDC (1 h pre-treatment) to effect an increase in $O_2^{\bullet-}$ rendered U2-OS cells resistant to chemotherapeutic drugs, Etoposide or Doxorubicin (24 h treatment) (Fig. 3A–D). To test if S62 phosphorylation of c-Myc was a critical factor in driving chemoresistance upon an increase in $O_2^{\bullet-}$, we employed *c-Myc WT* and *c-Myc S62A* (mutant) plasmids along with the *pcDNA-Dest40* vector control. These were stably transfected into U2-OS cells and the stable incorporation of the plasmids was tested by SDS-PAGE (Fig. S1C). These stable cells were subsequently subjected to Etoposide/Doxorubicin treatment for 24 h. As expected, DDC pre-treatment (1 h) was unable to rescue chemotherapy-induced cell death in the S62A c-Myc mutant (Fig. 3E and F). Likewise, a cell numbers assay was performed using the stable cell lines and, as is evident, only the S62A mutant failed to acquire DDC (1 h pre-treatment) mediated resistance to etoposide (24 h) induced cell death (Figs. S3A–S3D). Along similar lines, pre-treatment with MnTE-PyP5$^+$ (2 h pre-treatment), an SOD mimetic, was unable to potentiate enhanced cell death only for the S62A c-Myc mutant cell line when subjected to etoposide or doxorubicin (24 h) treatments (Fig. 3E and F). Subsequently, our BrDU cell proliferation assay also indicated that while DDC (1 h pre-treatment) was able to protect against the inhibition of cell proliferation by etoposide (24 h) in both U2-OS cells and WT c-Myc stable cells, the non-phosphorylatable S62A c-Myc overexpressing stable cells were not protected by $O_2^{\bullet-}$ against etoposide mediated inhibition of cell proliferation (Fig. 3G and H).

In addition, recent studies have indicated that metabolic plasticity of cancer cells wherein there exists a hybrid population of glycolytic and OXPHOS driven cells boosts tumor metabolism and drives

carcinogenesis [30–32]. In line with such observations, not only do we see an increase in glycolytic products (Fig. S2B), but furthermore, we provide evidence that cells carrying the mutant S62A exhibited significantly lower OCR and ECAR compared to the WT c-Myc overexpressing cells, which had measurably higher OCR and ECAR, compared to the vector counterpart, as analyzed by the Seahorse XF Analyzer (Fig. 3I). Together, these data provide testimony that the survival promoting effect of an increase in intracellular $O_2^{\bullet-}$ is a function of sustained S62 phosphorylation of c-Myc, which also correlates with the increased metabolic activity associated with c-Myc activation.

2.4. Superoxide prevents ubiquitination of c-Myc via its PP2A inhibition mediated phosphorylation

To ascertain the mechanism of stabilization of c-Myc in response to an increase in intracellular $O_2^{\bullet-}$, we first looked at the transcription and post-translational regulation of c-Myc. Pre-treatment of cells with the transcription inhibitor, Actinomycin D, did not deter DDC-induced stabilization of c-Myc (Figs. 4A and S4A), thus indicating that the effect of an increase in $O_2^{\bullet-}$ was not a result of increased transcription in our model system. Next, we questioned whether the effect of an increase in intracellular $O_2^{\bullet-}$ on c-Myc stability was a function of an increase in protein half-life and/or delayed degradation of the protein by the 26S proteasome. Using cycloheximide, a known protein translation elongation inhibitor, we were able to map the half-life of c-Myc in the presence and absence of DDC at various time points. Using the formula for exponential decay of protein, the half-life of c-Myc protein was delayed to roughly ~63 min in the presence of DDC as opposed to roughly ~27 min in the presence of cycloheximide alone (Fig. 4B and C and S4B).

To further highlight the contribution of the S62 phosphorylation of c-Myc towards the stabilization of the c-Myc oncoprotein, we employed the c-Myc overexpressing (WT c-Myc) and non-phosphorylatable c-Myc (S62A) stable cell lines and challenged them with cycloheximide in the presence and absence of DDC, identical to the experimental protocol for Fig. 4B. Clearly, our results demonstrated that while DDC was able to rescue the destabilization of c-Myc in the presence of cycloheximide in the WT c-Myc overexpressing cells; this was not observed in the S62A c-Myc mutant cell line, which was further refractory to DDC treatment (Fig. 4D).

In order to map protein ubiquitination and degradation we generated stable clones of U2-OS cell line harboring an HA-tagged Ubiquitin plasmid. Hereafter, we subjected cells to DDC or DPI treatment to modulate intracellular $O_2^{\bullet-}$ levels. While treatment of cells with DDC (4 h) was able to significantly inhibit the ubiquitination of c-Myc protein, DPI treatment (18 h) led to increased c-Myc ubiquitination (Fig. 4E and F). Moreover, when we subjected cells to treatment with the proteasome inhibitor in the presence or absence of DPI, which blocks $O_2^{\bullet-}$ production, we observed that, while DPI mediated destabilization of c-Myc could be rescued by the proteasome inhibitor MG132, DPI treatment continued to lead to dephosphorylation at S62 in the MG132 treated cells, thereby suggesting that S62 phosphorylation can be attributed to affecting the stability of c-Myc (Fig. S4C).

Since increasing concentrations of $O_2^{\bullet-}$ led to an increase in phosphorylation of c-Myc, we looked at the potential activation of kinases, ERK and JNK, known to phosphorylate c-Myc at S62. Firstly, DDC mediated increase in c-Myc stabilization was congruently accompanied with a rapid decline in the activation of ERK as mapped by its phosphorylation (Fig. S4D). Next, treatment with the pharmacological inhibitor of JNK or siRNA directed against *JNK* was unable to effect DDC-induced increase in c-Myc phosphorylation and stabilization (Figs. S4E and S4F). Having ruled out the involvement of kinases, we logically asked if this effect could be a function of PP2A inhibition.

2.5. Superoxide inhibits PP2A holoenzyme assembly

To delineate the mechanism behind c-Myc phosphorylation in cells having augmented $O_2^{\bullet-}$ levels, we next looked at the phosphatase responsible for regulating S62 c-Myc phosphorylation. Notably, PP2A activity was modestly inhibited in the presence of DDC (4 h), whereas DPI (18 h) treatment robustly increased PP2A activity (Fig. 5A). This led us to question how PP2A activity on c-Myc was indeed affected by intracellular $O_2^{\bullet-}$ concentrations.

In line with previous reports, treatment with discrete *B56* siRNA (48 h) sequences determined that only in the *B56α* siRNA treated cells, c-Myc phosphorylation was sustained (S62) and the protein stabilized (Fig. 5B). Correspondingly, transient transfection of the *B56α* subunit corresponded with effective dephosphorylation at S62 and destabilization of c-Myc, which could be rescued by subsequent treatment with DDC for 4 h (Fig. 5C). Of note, c-Myc was found to interact with PP2A B56α and this was also subtly increased upon DDC (4 h) treatment (Fig. 5D). Moreover, endogenous PP2A C immunoprecipitation indicated enhanced interaction with c-Myc in DPI (18 h) treated cells (Fig. 5E). Finally, both blocking $O_2^{\bullet-}$ production or scavenging $O_2^{\bullet-}$ in U2-OS cells resulted in greater interaction of B56α and PP2A C. This was witnessed when immunoprecipitation of PP2A C in the presence of DPI (18 h) implicated greater interaction with the B56α subunit of PP2A and correspondingly the immunoprecipitation of HA tagged B56α subunit of PP2A demonstrated an increase in interaction with PP2A C in the presence of Tiron (5 h) (Fig. 5F and G). Collectively, these results lend support to the hypothesis that $O_2^{\bullet-}$ dependent modulation of c-Myc stability (via sustained S62 phosphorylation) and activity is a function of PP2A inactivation.

2.6. Peroxynitrite formed downstream of $O_2^{\bullet-}$ is critical in phospho-stabilization and activation of c-Myc

Intracellular $O_2^{\bullet-}$ is either converted to H_2O_2 by the various SODs or reacts with nitric oxide (NO) to generate the highly reactive peroxynitrite ($ONOO^-$). In this study intracellular $O_2^{\bullet-}$ was amplified by inhibiting its dismutation (SOD1-mediated) to H_2O_2. Moreover, we already confirmed that H_2O_2 did not affect c-Myc phospho-stabilization (Fig. S2D). To ascertain if $ONOO^-$ was responsible for the sustained S62 phosphorylation of c-Myc, we first employed pharmacological inducers of NO as well as exogenous addition of pure $ONOO^-$. Indeed, exposure of U2-OS cells to SNP (6 h) or $ONOO^-$ (2 h) significantly upregulated c-Myc phospho-stabilization as well as reporter activity (Fig. 6A and B). Similar effects were observed with SIN-1 (6 h), another NO modulator (Fig. S5A). Subsequent treatments with L-NAME in U2-OS cells (1 h pre-treatment), which impedes NO production, and FeTPPS (2 h pre-treatment), a $ONOO^-$ decomposition catalyst in U2-OS and PANC-1 cells, resulted in a marked decrease in c-Myc stabilization effected by DDC (4 h) (Fig. 6C and D). L-NAME treatment (1 h pre-treatment) was also able to markedly reduce c-Myc activation induced by DDC (4 h) (Fig. S5B). Finally, the enhanced stabilization and S62 phosphorylation of c-Myc induced upon gene knockdown of *SOD1* (siSOD1/24 h) was remarkably inhibited upon treatment with FeTPPS (6 h) (Fig. 6E). More importantly, while $ONOO^-$ treatment (2 h) strongly inhibited c-Myc ubiquitination, FeTPPS treatment (6 h) was able to markedly enhance c-Myc ubiquitination (Fig. 6F and G).

2.7. Peroxynitrite-mediated nitration of B56α subunit impedes PP2A holoenzyme assembly

Next, we sought to understand the mechanism by which the increase in $ONOO^-$ levels led to PP2A inhibition. S-nitrosylation of cysteine residues and nitration of tyrosine residues are the two modes by which $ONOO^-$ targets proteins. It is unlikely that $ONOO^-$ targets the residues of the core enzyme (A/C subunits of PP2A) as this would lead to global inhibition of PP2A activity and thus have a severe impact on

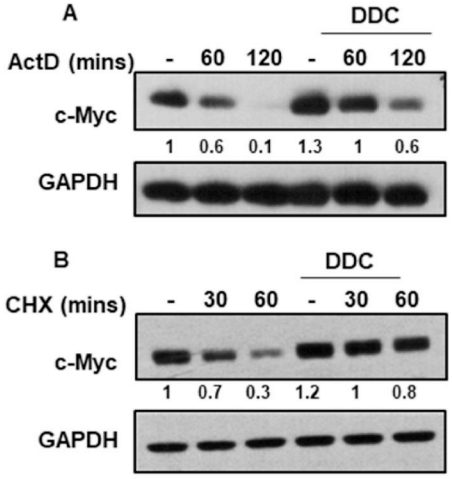

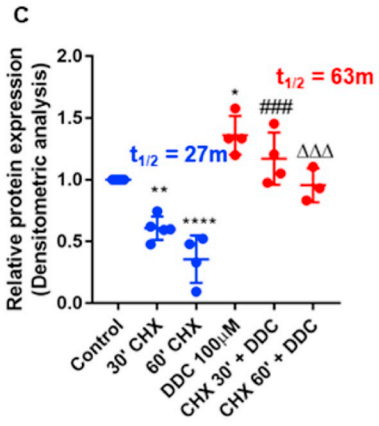

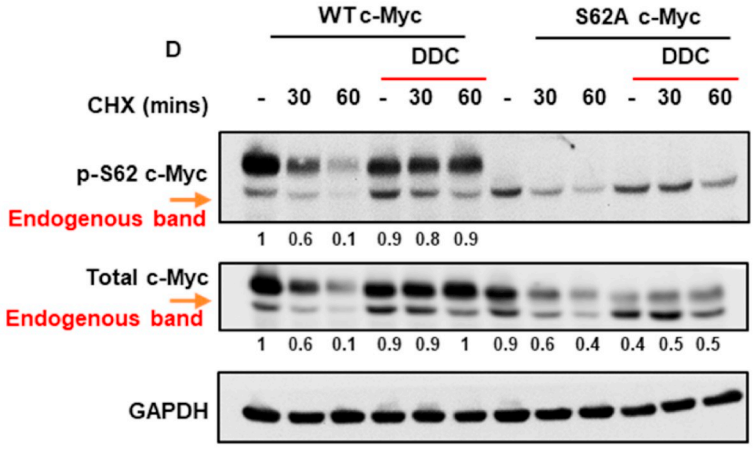

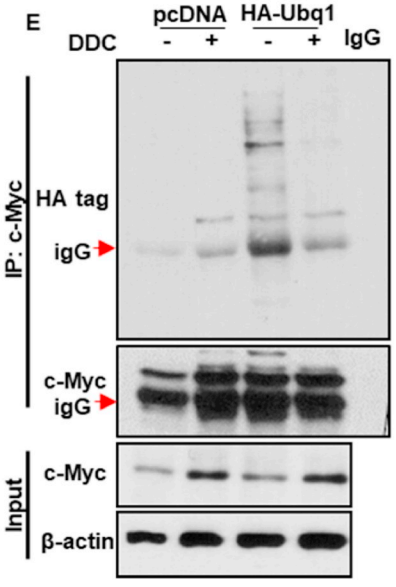

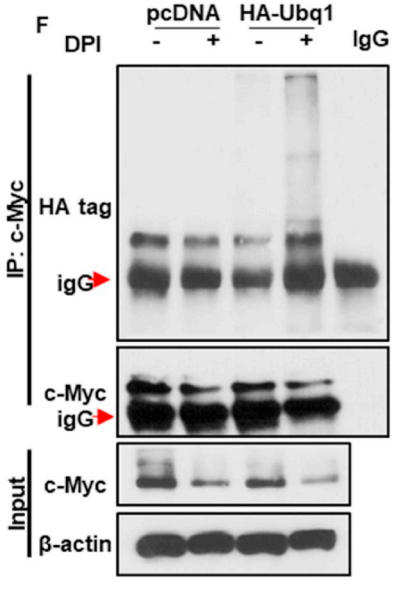

(caption on next page)

Fig. 4. ***Superoxide stabilizes c-Myc via its S62 phosphorylation by preventing its polyubiquitination.*** (A and B) Western blot analyses of total c-Myc protein. Cells were subjected to actinomycin D or cycloheximide treatment in the presence or absence of DDC (100 μM) treatment. (C) Densitometric analysis of cells chased with cycloheximide and calculation of c-Myc half-life in the presence and absence of secondary DDC treatment. Half-life is calculated as per the equation: $Y = Ni\ exp(-\lambda t)$; Half-life $= \ln 2/\lambda$ (D) WT c-Myc and S62A c-Myc overexpressing cell lines (U2-OS) were subjected to cycloheximide treatment in the presence or absence of DDC (100 μM) treatment. Higher bands reflect the transfected c-Myc protein, while the lower bands represent the endogenous c-Myc protein. (E and F) Ubiquitination IP assay analysis by Western blot to determine the level of c-Myc ubiquitination in the presence and absence of DDC (100 μM/4 h) or DPI (5 μM/18 h) treatments. T-test was employed for statistical analysis (* = $p < 0.05$, ** = $p < 0.01$, $^{###}$ = $p < 0.001$, $^{\Delta\Delta\Delta}$ = $p < 0.001$, **** = $p < 0.0001$; $^{###}$ and $^{\Delta\Delta\Delta}$ determine significance against 30′CHX and 60′CHX treatments respectively).

the proteome, which was not observed in our model (Fig. 5A). Therefore, we focused on the regulatory subunit B56α. Again, impacting the binding of B56α to c-Myc was not considered as a mechanism as in Fig. 5D, we clearly observed that this interaction was not diminished by DDC treatment. Therefore, we hypothesized that $ONOO^-$ might affect holoenzyme assembly of PP2A by impacting the interaction of c-Myc bound B56α to PP2A A/C core enzyme. Importantly, no cysteine residue on B56 subunit was deemed essential for binding the PP2A A/C core enzyme. However, tyrosine residue (Y238) on B56α was implicated in binding to the PP2A A subunit [33,34]. Protein tyrosine nitration is strictly commanded by specific criteria that govern the susceptibility of the tyrosine residue to nitrative modifications. Serendipitously, our in-silico analysis determined that these criteria [54] complemented the location of Y238 residue (Figs. S6A–S6C).

Therefore, we set out to investigate whether B56α Y238 residue was nitrated by $ONOO^-$. To do so, lysates immunoprecipitated with anti-B56α were probed for 3-nitrotyrosine modification. Corroborating our hypothesis, B56α was indeed nitrated upon exposure to DDC (4 h) (Fig. 7A). Subsequently, we employed the proximity ligation assay (PLA) to examine the interaction of PP2A B56α with the scaffold PP2A A subunit. Our results showed an impaired interaction between PP2A A and B56α in cells treated with DDC (4 h), but in contrast an enhanced interaction between the two proteins was observed in the presence of FeTPPS (6 h) (Fig. 7B). Next, we performed site directed mutagenesis to mutate Y238 to the non-nitratable phenylalanine Y238F B56α (Fig. 7C). The mutant Y238F B56α was insensitive to nitration and was therefore incompetent in phospho-stabilization and activation of c-Myc imparted by DDC treatment (4 h) as compared to the wild-type counterparts (Fig. 7D and E). Finally, the mutant Y238F B56α was found to constitutively interact with the catalytic subunit of PP2A and insensitive to the action of DPI (18 h) in mediating this interaction (Fig. S6D). Moreover, transient overexpression of the non-nitratable Y238F B56α plasmid in U2-OS cells led to the constitutive dephosphorylation of c-Myc at the S62 residue as well as its constitutive destabilization, which were insensitive to both DDC (4 h) and $ONOO^-$ (2 h) insults (Figs. S6E and S6F). Taken together, these data argue in favor of $ONOO^-$-mediated nitration of B56α sub-unit in disrupting PP2A holoenzyme assembly, thus leading to the phospho-stabilization and activation of its substrate protein c-Myc (Fig. 7F).

3. Discussion

3.1. c-Myc activation regulated by the redox milieu favors pro-tumorigenic programs in cancer cells

Redox dependent signaling is yet a nascent field and the idea that the pro-oxidant milieu is intricately associated with tumor aggressiveness is gaining momentum. Deregulated c-Myc overexpression is a common factor in driving tumor progression and rendering cancers refractory to standard chemotherapeutics. It is therefore critical to understand the molecular mechanisms through which aberrant c-Myc expression in cancers contributes to these phenotypes. Therefore, through modulation of c-Myc stabilization and phospho-activation, the intracellular redox milieu can be viewed as a critical determinant of cell fate decisions. The concurrent association of a redox tumor landscape and deregulated c-Myc activation in cancers prompted us to question the role of the intracellular redox milieu in characterizing c-Myc driven oncogenic programs in cancer cells. Indeed, several studies have indicated a positive impact of c-Myc and its isoforms in the induction of ROS either through modulation of mitochondrial function and subsequently the ETC or counterintuitively towards balancing the damaging effects of ROS through impinging its regulation on proteins such as HIF-1α and peroxiredoxin 3, which buffer the redox impact [35–38].

To characterize the impact of a pro-oxidant microenvironment on the c-Myc oncoprotein, we employed several pharmacological compounds as well as knock-down approaches to modulate intracellular $O_2^{\bullet-}$ levels. Our results clearly indicate that an increase in intracellular $O_2^{\bullet-}$ was concurrent with stabilization of c-Myc protein as well as its phosphorylation at S62 residue, which increases its transactivation potential. Moreover, such transactivation was accompanied with increased expression of c-Myc transcriptional targets as well as a coordinated increase in the chemoresistance potential of osteosarcoma cells, which was critically dependent on S62 phosphorylation of c-Myc. At this juncture, it is to be noted that our observations have uncovered a novel pathway for redox dependent post-translational stabilization of c-Myc. However, we must proceed with caution to elaborate the same pathway on other solid tumor cell types. While, we do note redox dependent regulation of both the phospho S62 c-Myc as well as total c-Myc protein in our Western blot assays for some cell lines (Fig. 1B, 1F and 1H), studies to look at the *c-Myc* mRNA expression in these cells is underway. Earlier studies have indeed potentiated a role for $O_2^{\bullet-}$ mediated transcriptional upregulation of *c-Myc* in cancers. For example, one study suggested that *c-Myc* modulation in response to elevated $O_2^{\bullet-}$ was an indirect consequence of NF-κB activation-which leads to upregulation of its transcriptional target *c-Myc*-by correlating *c-Myc* expression with NF-κB activation [39]. Another study implied that *c-Myc* mRNA was induced by cadmium in response to increases in intracellular $O_2^{\bullet-}$ and H_2O_2, however, the phenotype was evident only in 40% of the samples [40]. Collectively, the precise molecular mechanisms underlying the potentiating effect of an increase in intracellular $O_2^{\bullet-}$ on c-Myc phospho-stability remains poorly described. This report is the first to offer a mechanistic insight by which intracellular $O_2^{\bullet-}$ modulates c-Myc protein stabilization and activity.

3.2. Redox dependent modulation of c-Myc at the post-translational level is a consequence of $ONOO^-$ accumulation mediated inhibition of PP2A

Superoxide anion is a short-lived radical in cells with a half-life of a few seconds. Therefore, at physiological pH, its biological activity in cellular physiology is extremely limited and it is either spontaneously dismutated by SOD enzymes to H_2O_2 or converted to $ONOO^-$ upon its reaction with NO, a product of iNOS. In our model, c-Myc upregulation could be induced through increase in intracellular $O_2^{\bullet-}$ concentration meted through blocking its dismutation. This led us to investigate the role of $ONOO^-$ in altering c-Myc protein expression and activity. In agreement with our hypothesis, $ONOO^-$ was critical in inducing the stabilization and phosphorylation of c-Myc at S62 residue. Our observations highlight the delicate physiological balance between the two enzymes SOD and iNOS in determining the fate of $O_2^{\bullet-}$ mediated signaling. In our model, we did not identify transcriptional upregulation of *c-Myc* expression in response to the pro-oxidant milieu. Instead our actinomycin D and cycloheximide chase experiments as well as our

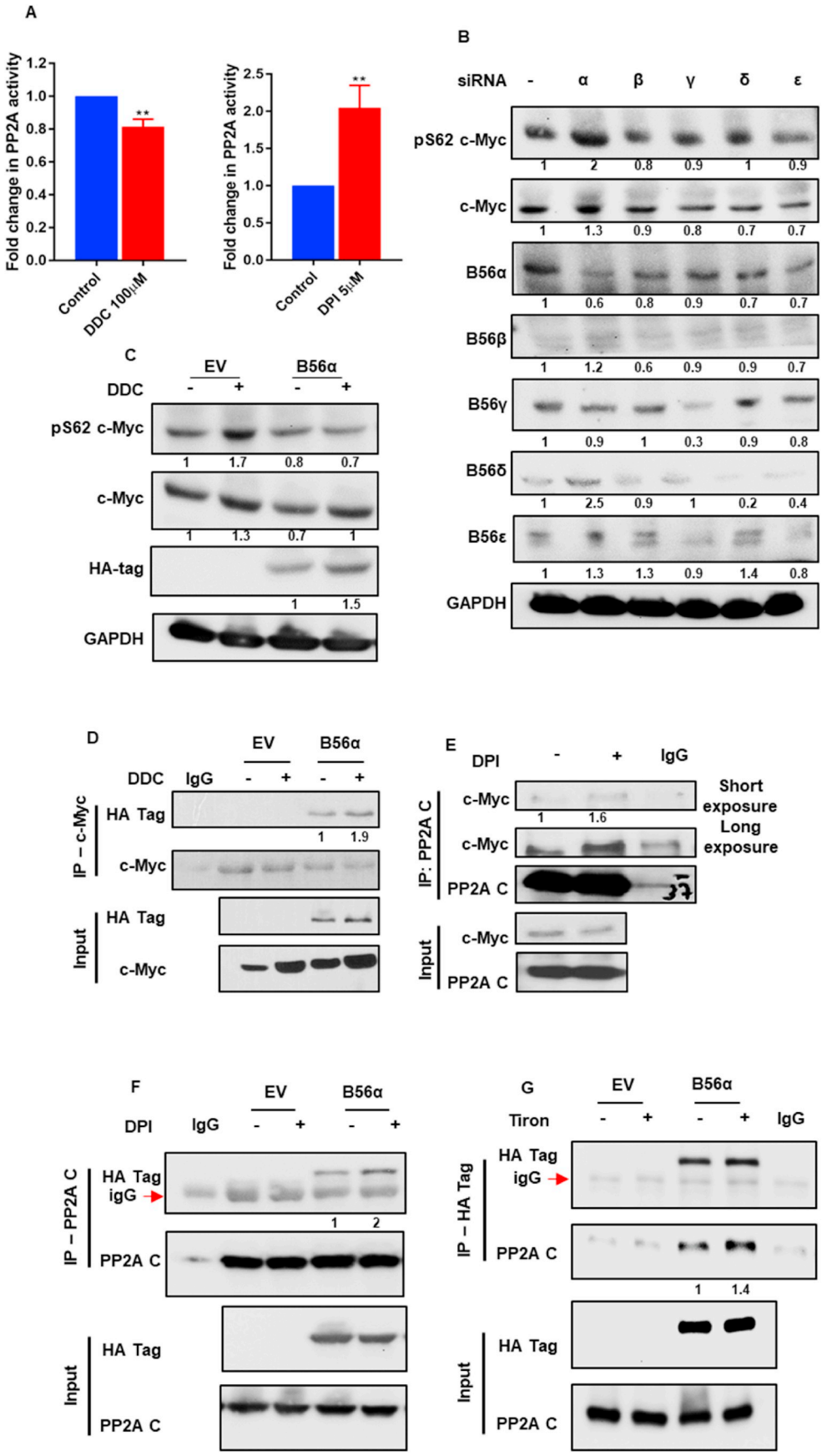

Fig. 5. ***Superoxide regulates c-Myc by inhibiting PP2A mediated dephosphorylation.*** (A) PP2A activity assay of U2-OS cells when challenged with DDC (100 μM/4 h) or DPI (5 μM/18 h). (B) U2-OS cells were challenged with siRNA (100 nM/48 h) targeted against individual B56 isoforms and subjected to Western blot analyses to ascertain change in S62 c-Myc phosphorylation and total c-Myc stabilization. (C) U2-OS cells were transfected with HA tagged B56α and analyzed by Western blot for pS62 c-Myc and total c-Myc protein levels in response to DDC (100 μM/4 h) treatment. (D) Immunoprecipitation of c-Myc demonstrates its interaction with the HA tagged B56α subunit of PP2A in response to DDC (100 μM/4 h) treatment. (E) Immunoprecipitation of PP2A C indicates higher interaction of c-Myc with catalytic subunit of PP2A in the presence of DPI (5 μM/18 h). (F) Immunoprecipitation of PP2A C demonstrates higher interaction with HA tagged B56α subunit of PP2A in the presence of DPI (5 μM/18 h). (G) Immunoprecipitation of HA tagged B56α subunit of PP2A indicates higher interaction of c-Myc with catalytic subunit of PP2A in the presence of Tiron (5 mM/5 h). T-test was employed for statistical analysis (** = $p < 0.01$).

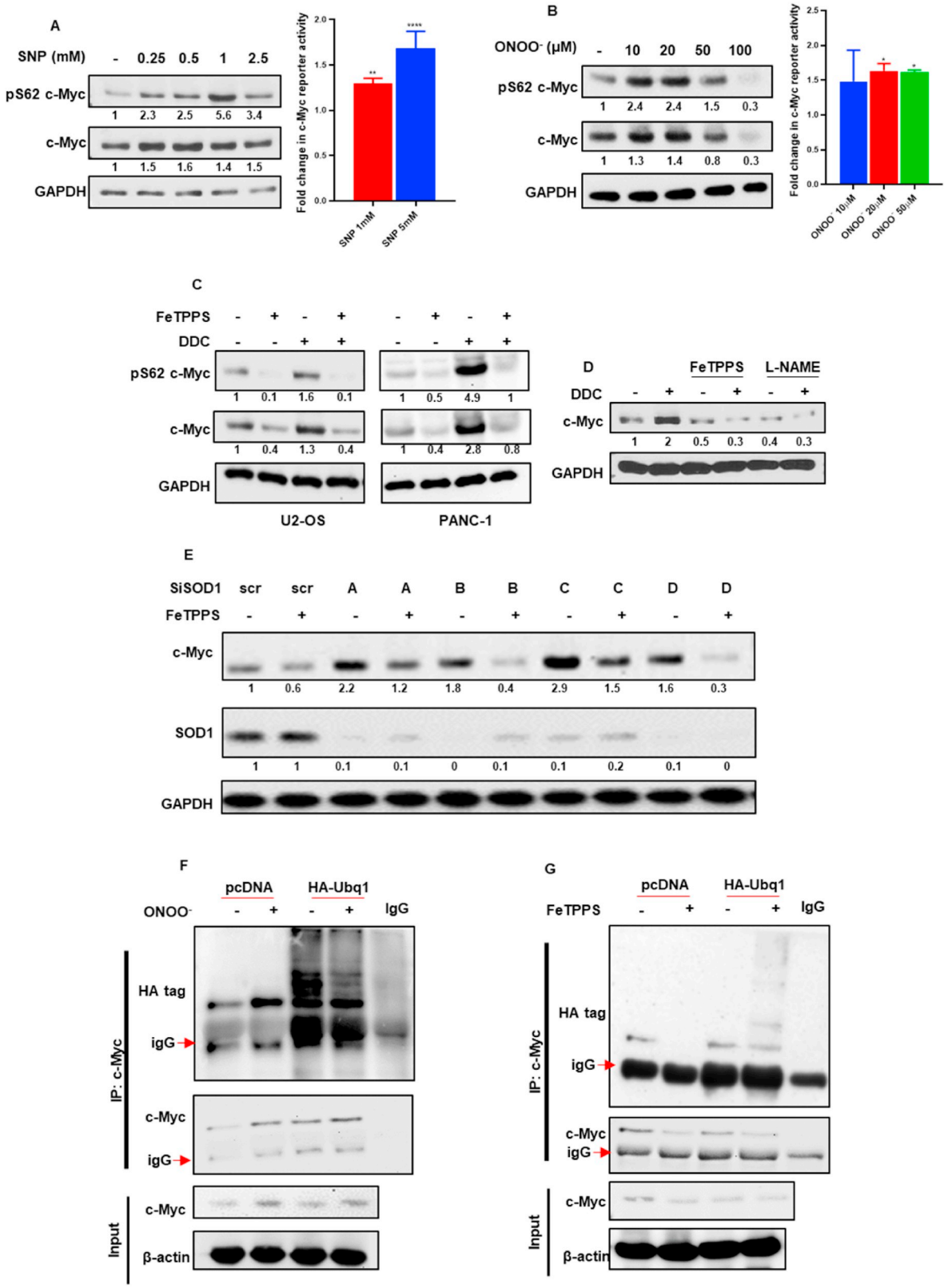

Fig. 6. ***Peroxynitrite mediated inhibition of PP2A activity is responsible for c-Myc stabilization and phospho-activation.*** (A and B) Western blot and c-Myc reporter luciferase analyses of U2-OS cells subjected to SNP (6 h) and peroxynitrite (2 h) treatments. Fold change in c-Myc reporter activity was normalized to vehicle control. (C and D) Western blot analyses in U2-OS cells of pS62 c-Myc and total c-Myc in the presence of FeTPPS (100 μM/2 h pre-treatment) and L-NAME (5 mM/1hr pre-treatment) with DDC (100 μM/4 h) treatments. (E) Western blot analyses of U2-OS cells subjected to siRNA (100 nM/24 h) targeted against SOD1 demonstrates elevated c-Myc levels which are subsequently depleted in the presence of FeTPPS (100 μM/6 h). (F and G) Ubiquitination IP assay analysis by Western blot to determine the level of c-Myc ubiquitination in the presence and absence of peroxynitrite (20 μM/2 h) or FeTPPS (100 μM/6 h) treatments. One-way ANOVA was employed for statistical analysis (* = $p < 0.05$, ** = $p < 0.01$, **** = $p < 0.0001$).

ubiquitination assays supported the argument that $O_2^{\bullet-}$ and $ONOO^-$ dependent modulation of c-Myc protein is effected through the regulation of c-Myc proteolysis. We limited our focus to the Fbw7 ubiquitin ligase as it has been demonstrated to recognize the phosphodegron ($PT^{58}PPLS^{62}$) in the transactivation domain of c-Myc [41,42]. Notably, when we blocked degradation with MG132, we observed that DPI-

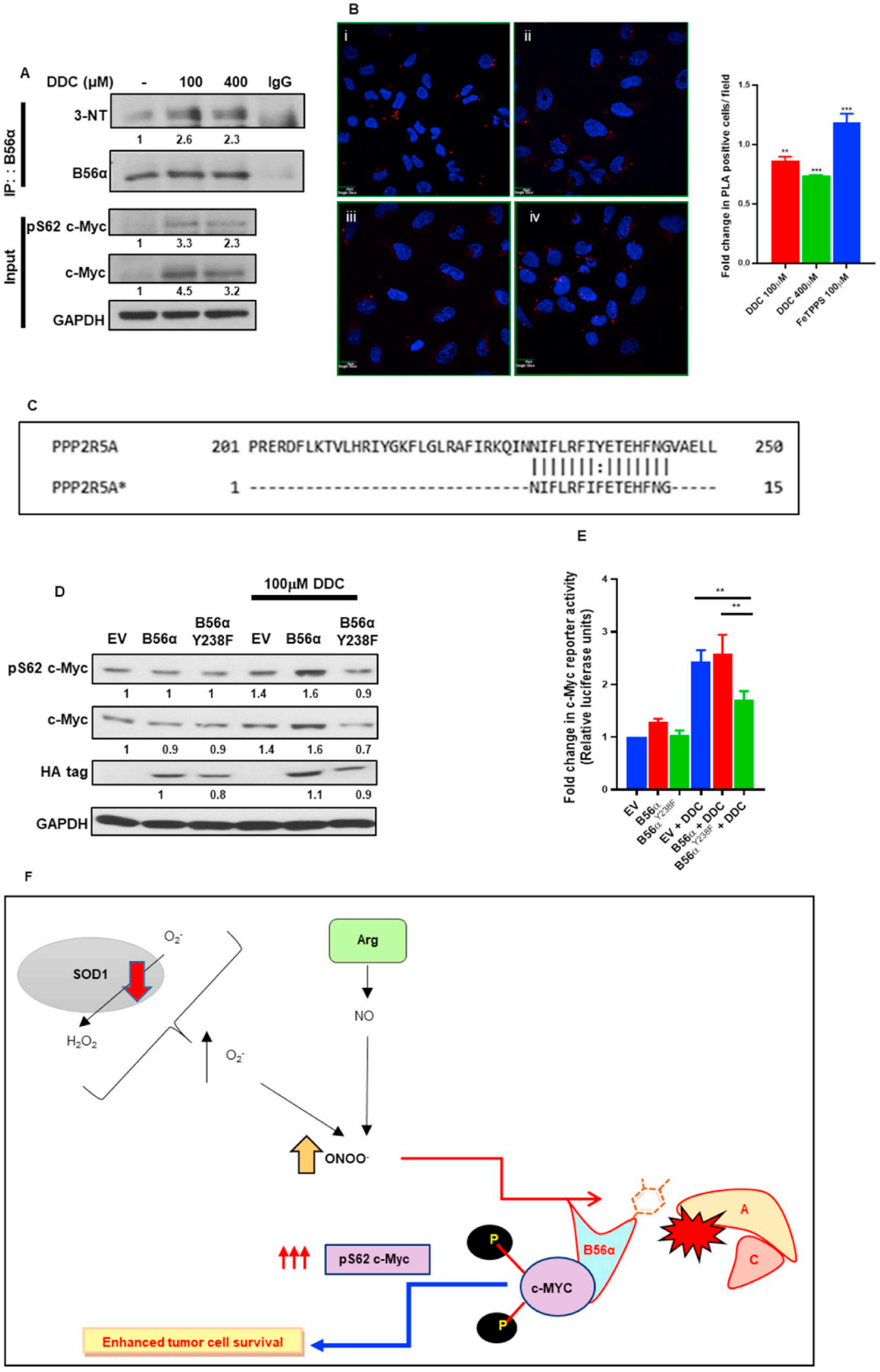

(caption on next page)

Fig. 7. ***Peroxynitrite disrupts PP2A holoenzyme assembly by nitration of B56α at the Y238 position:*** (A) Immunoprecipitation of B56α demonstrated increased 3-nitrotyrosine mark in the presence of DDC treatment in PANC-1 cells. (B) PLA assay demonstrates decreased interaction between scaffold subunit PP2A-A and B56α when U2-OS cells were subjected to DDC treatments (4 h), whereas treatment with FeTPPS (6 h) demonstrates a reciprocal increase in interaction (i – Control, ii – DDC 100 μM, iii – DDC 400 μM, iv – FeTPPS 100 μM). (C) Primer design for site-directed mutagenesis of B56α Y238 to non-nitratable phenylalanine. (D) Western blot analyses of pS62 c-Myc and total c-Myc protein levels in EV, B56α and B56αY238F mutant cells in the presence of DDC (100 μM/4 h). (E) c-Myc reporter luciferase activity assay analyses of EV, HA tagged B56α and HA tagged B56αY238F mutant cells subjected to DDC (100 μM/4 h) treatment. Fold change in c-Myc reporter activity was normalized to EV control. (F) Summary graphical model of pro-oxidant redox dependent stabilization and activation of c-Myc oncoprotein in cancer cells – Mild increase in superoxide levels is followed by a rise in intracellular peroxynitrite levels, which leads to nitrative inhibition of B56α at the Y238 position, subsequently resulting in the sustained phospho-stabilization and activation of c-Myc, which drives the oncogenic programs in the tumor cells. One-way ANOVA was employed for statistical analysis (** = $p < 0.01$, *** = $p < 0.001$).

mediated destabilization of c-Myc was a consequence of dephosphorylation of c-Myc at the S62 residue. In congruence with earlier reports, we observed that c-Myc stabilization in our model was indeed associated with a concomitant increase in the stabilizing S62 phosphorylation of c-Myc. Therefore, we shifted our attention to the kinases, ERK and JNK, and phosphatase PP2A, which have been reported to regulate c-Myc phosphorylation at the S62 residue [14,43,44]. In this direction, our observations suggested a role for the pro-oxidant microenvironment in inhibition of the phosphatase PP2A. PP2A is a ubiquitous broad specificity serine/threonine (S/T) phosphatase comprising of the core A-C enzyme and the independent B regulatory subunits. The diversity and substrate specificity of the B regulatory subunit provides for the assembly of more than 200 types of biochemically distinct heterotrimeric PP2A holoenzyme, which underlies the justification for the exhaustive number of proteins that are dephosphorylated by the singular holoenzyme complex [45,46]. Numerous studies have now acknowledged the prominent role of PP2A as a bonafide tumor suppressor protein highlighted through its mutation/inactivation contributing to tumor exacerbation [47–52]. Moreover, key substrates of PP2A include onco-proteins whose dephosphorylation impairs stability and/or activity of these proteins; while dephosphorylation of some tumor suppressor substrates leads to their activation [53]. PP2A phosphatase is particularly an interesting target as we have recently demonstrated that one arm of the PP2A phosphatase is subject to redox-mediated inhibition [11,54].

To understand the nature of inhibition of PP2A effected through an increase in intracellular $ONOO^-$ levels, we focused on the molecular function of the RNS in cellular physiology. Peroxynitrite can intrinsically modulate protein activity through post-translational modifications leading to enzymatic or physical alterations through nitration of tyrosine residues or through S-nitrosylation of cysteine residues. The role of $ONOO^-$ in cancers is dichotomous with studies suggesting that mild increase in physiological concentrations of $ONOO^-$ promote carcinogenesis, whereas high levels in cells can lead to adverse consequences [55,56]. In 2006–2007, Xu et al., published successive papers on the crystal structure of the heterotrimeric PP2A complex, wherein they specifically highlighted the different residues on B56 regulatory subunit deemed necessary for binding with the PP2A A/C core enzyme [33,34]. In our model, we identified $ONOO^-$ to disrupt PP2A holoenzyme assembly. In agreement with our in-silico analysis, we identified the Y238 residue of B56α to be nitration labile. Nitration of the B56α subunit further restricted the interaction of the B regulatory subunit with the core enzyme, leading to disruption of the heterotrimeric complex and ensuing in the sustained phosphorylation, stabilization and activation of c-Myc in the pro-oxidant microenvironment.

The clinical relevance of SOD1 expression in cancers and its potential reciprocal expression in comparison to S62 c-Myc phosphorylation as well as nitration of B56α Y238 may aid in diagnostic stratification of osteosarcomas and other solid tumors. While SMAPs stand for small molecule activators of PP2A which have been demonstrated to bind the scaffold A subunit of PP2A and subsequently boost holoenzyme assembly [57], presenting the plausibility of competing with tyrosine nitration mediated disruption of holoenzyme formation; SOD mimetics serve to behave like superoxide dismutase enzymes by harboring a metal-centric positive charge and thus augment the redox cycling of negatively charged ROS species. It would therefore be interesting to evaluate the therapeutic potential of these compounds in the reactivation of PP2A and/or alleviating ROS/RNS mediated effects on PP2A and c-Myc in solid tumors.

In summary, our work has identified a novel mechanism wherein the redox milieu is mechanistically able to modulate c-Myc stabilization and activation in solid tumors through the nitrative modification of PP2A B56α, leading to loss of c-Myc phosphatase PP2A assembly. We have further demonstrated that the pro-oxidant mediated increase in the oncogenic functions of c-Myc are directly governed by its phosphorylation at the S62 residue. This, therefore, presents with an attractive opportunity to tailor therapeutic interventions to target this novel signaling node to alleviate c-Myc driven carcinogenesis.

4. Methods

Coimmunoprecipitation assay: Cells were lysed with co-IP lysis buffer and stored overnight at −80 °C. 1.2–1.5 mg of freeze thaw lysates were subjected to preclearing with protein A or protein G agarose beads (Santa Cruz, Texas, USA), based on the primary IP antibody. 3–4 μg of primary antibody was added to all samples, while normal IgG was added to the IgG control. All samples were subjected to constant mixing on the rotor overnight at 4 °C, and further immunoprecipitated with the respective agarose beads. Subsequently, beads were washed three times with co-IP buffer followed by boiling for 20 min with loading dye.

Immunofluorescence confocal microscopy: Cells were fixed on coverslips with 4% PFA and subjected to gentle lysis with 0.2% Triton-X. Coverslips were then blocked in BSA before incubation overnight with the c-Myc antibody at 4 °C. Subsequently, cells were incubated with 1:200 dilution of Alexafluor-568 anti-rabbit secondary antibody (Invitrogen, California, USA). The cover slips were then transferred to slides with DAPI mounting medium. Images were captured with Olympus Fluoview-FV1000 (Tokyo, Japan) confocal microscope.

Duolink PLA Assay: The Duolink PLA assay was purchased from Sigma Aldrich (Missouri, USA). Briefly, cells were grown on coverslips and then fixed in 4% PFA followed by permeabilization with 0.2% Triton-X. Subsequent steps were performed according to manufacturer's instructions. Images were captured with Olympus Fluoview-FV1000 (Tokyo, Japan) confocal microscope. At least 20 fields were scored in each experiment.

MTT cell viability assay: Cells were plated in a 6-well plate, 24 h prior to treatments. After media was refreshed, cells were subjected to respective treatments at 70% confluency and left for 24 h as described in results. Cells were then harvested as usual with trypsin. All media was collected. A 1:1 mixture of cells with 4 mg/mL MTT was plated in triplicates on a 96-well format transparent plate and incubated for 2 h at 37 °C. The plate was then spun down at 4500 RPM/20 min and the violet formazan crystals were dissolved in DMSO. Cell viability was then quantitated spectrophotometrically at an absorbance wavelength of 570 nm using TECAN spectrophotometer.

Crystal violet cell viability colony forming assay: Cells were treated with DDC, an hour prior to treatment with standard chemotherapeutic agents. 24 h later, cells were trypsinised and 4000 cells were plated onto a new plate and colonies were allowed to form over a

period of 8–10 days. Cells were subsequently washed with 1X PBS and incubated with crystal violet solution for 20 min at RT. The plates were then washed off with water and the images were captured with the ChemiDoc (Thermoscientific, Massachusetts, United States) thereafter. The Clono-Counter software was employed to generate counts for the colony forming assay [58].

Lucigenin chemiluminescence assay: Cells were trypsinised and harvested in 450 μl of ATP releasing buffer at room temperature. Chemiluminescence was determined instantaneously at 0.5 s intervals for a total of 30 s using the Berthold Sirius Luminometer (Bad Wildbad, Germany) which auto-injected Lucigenin reconstituted in PBS into the samples The resultant values for each sample were averaged over time and normalized by protein concentration of the remaining lysate.

BrDU cell proliferation assay: The BrdU Cell Proliferation Assay Kit was purchased from Cell Signaling Technology (Massachusetts, United States). Briefly, 5000 cells were plated in a 96-well plate in triplicates. Cells were treated with DDC, an hour prior to treatment with Etoposide. Following 24 h incubation, cells were pulsed with BrDU for 3 h. Subsequent steps were carried out using manufacturer's instructions. The absorbance was measured at 450 nm using a TECAN spectrophotometer (Männedorf, Switzerland).

c-Myc reporter Luciferase assay: The Cignal Myc Reporter (luc) Kit was purchased from SABiosciences (Qiagen, Hilden, Germany). The kit contains three luciferase tagged plasmids: c-Myc reporter construct as well as optimised positive and negative controls. 15 ng of each plasmid was transfected the day after plating into 48-well plates in triplicates by the calcium phosphate delivery method. The Promega (Wisconsin, USA) Dual Luciferase Reporter assay kit was employed for detecting firefly and renilla luciferase activities using a 96-well white bottom plate to read luminescence with the Varioskan LUX Multimode Microplate Reader (Thermoscientific, Massachusetts, United States).

Authorship contribution

SP conceptualized the study. DR conducted most of the experiments. DR and SP wrote the manuscript. SC provided help with the design of experiments and KI and JH provided help on the Seahorse XF analyser experiments.

Declaration of competing interest

The authors declare no potential conflicts of interest.

Acknowledgments

The authors thank Prof David M. Virshup who provided anti-B56α and anti-B56β antibodies as well as the V5-tagged c-Myc plasmid constructs, and critical guidance on the project, Prof Ines Batinic-Haberle for the MnTE 2-PyP5^{+} SOD mimetic compound, and Prof Marie V. Clement for her critical input on the project and manuscript. This work is supported by grants from the NCIS, NUHS, Singapore seed funding programme and National Medical Research Council of Singapore (grant numbers NMRC/CIRG/1433/2015 and NMRC/OFIRG/0041/2017) to SP.

Appendix A. Supplementary data

Supplementary data to this article can be found online at https://doi.org/10.1016/j.redox.2020.101587.

References

[1] M.V. Clément, I. Stamenkovic, Superoxide anion is a natural inhibitor of FAS-mediated cell death, EMBO J. 15 (2) (1996) 216–225.
[2] K. Irani, et al., Mitogenic signaling mediated by oxidants in ras-transformed fibroblasts, Science 275 (5306) (1997) 1649.
[3] J.J. Cullen, et al., The role of manganese superoxide dismutase in the growth of pancreatic adenocarcinoma, Canc. Res. 63 (6) (2003) 1297.
[4] D. Ferraro, et al., Pro-metastatic signaling by c-Met through RAC-1 and reactive oxygen species (ROS), Oncogene 25 (2006) 3689.
[5] S. Pervaiz, M.V. Clement, Superoxide anion: oncogenic reactive oxygen species? Int. J. Biochem. Cell Biol. 39 (7–8) (2007) 1297–1304.
[6] N. Aykin-Burns, et al., Increased levels of superoxide and H_2O_2 mediate the differential susceptibility of cancer cells versus normal cells to glucose deprivation, Biochem. J. 418 (1) (2009) 29–37.
[7] F. Weinberg, et al., Mitochondrial metabolism and ROS generation are essential for Kras-mediated tumorigenicity, Proc. Natl. Acad. Sci. Unit. States Am. 107 (19) (2010) 8788–8793.
[8] M.V. Clement, J.L. Hirpara, S. Pervaiz, Decrease in intracellular superoxide sensitizes Bcl-2-overexpressing tumor cells to receptor and drug-induced apoptosis independent of the mitochondria, Cell Death Differ. 10 (11) (2003) 1273–1285.
[9] Z.X. Chen, S. Pervaiz, Bcl-2 induces pro-oxidant state by engaging mitochondrial respiration in tumor cells, Cell Death Differ. 14 (9) (2007) 1617–1627.
[10] R. Velaithan, et al., The small GTPase Rac1 is a novel binding partner of Bcl-2 and stabilizes its antiapoptotic activity, Blood 117 (23) (2011) 6214–6226.
[11] S.J.F. Chong, et al., A feedforward relationship between active Rac1 and phosphorylated Bcl-2 is critical for sustaining Bcl-2 phosphorylation and promoting cancer progression, Canc. Lett. 457 (2019) 151–167.
[12] S. Pervaiz, et al., Activation of the RacGTPase inhibits apoptosis in human tumor cells, Oncogene 20 (43) (2001) 6263–6268.
[13] J.L. Hirpara, et al., Superoxide induced inhibition of death receptor signaling is mediated via induced expression of apoptosis inhibitory protein cFLIP, Redox Biol. 30 (2020) 101403.
[14] R. Sears, et al., Multiple Ras-dependent phosphorylation pathways regulate Myc protein stability, Genes Dev. 14 (19) (2000) 2501–2514.
[15] K. Bhatia, et al., Point mutations in the c-Myc transactivation domain are common in Burkitt's lymphoma and mouse plasmacytomas, Nat. Genet. 5 (1) (1993) 56–61.
[16] E. Yeh, et al., A signalling pathway controlling c-Myc degradation that impacts oncogenic transformation of human cells, Nat. Cell Biol. 6 (4) (2004) 308–318.
[17] N. Popov, et al., Fbw7 and Usp28 regulate Myc protein stability in response to DNA damage, Cell Cycle 6 (19) (2007) 2327–2331.
[18] M.R. Junttila, J. Westermarck, Mechanisms of MYC stabilization in human malignancies, Cell Cycle 7 (5) (2008) 592–596.
[19] X. Wang, et al., Phosphorylation regulates c-Myc's oncogenic activity in the mammary gland, Canc. Res. 71 (3) (2011) 925–936.
[20] E. Yeh, et al., A signalling pathway controlling c-Myc degradation that impacts oncogenic transformation of human cells, Nat. Cell Biol. 6 (2004) 308.
[21] N. Gomez-Roman, et al., Direct activation of RNA polymerase III transcription by c-Myc, Nature 421 (6920) (2003) 290–294.
[22] A. Arabi, et al., c-Myc associates with ribosomal DNA and activates RNA polymerase I transcription, Nat. Cell Biol. 7 (3) (2005) 303–310.
[23] N. Gomez-Roman, et al., Activation by c-Myc of transcription by RNA polymerases I, II and III, Biochem. Soc. Symp. (73) (2006) 141–154.
[24] M.K. Mateyak, A.J. Obaya, J.M. Sedivy, c-Myc regulates cyclin D-Cdk4 and -Cdk6 activity but affects cell cycle progression at multiple independent points, Mol. Cell Biol. 19 (7) (1999) 4672–4683.
[25] Y. Fan, K.G. Dickman, W.-X. Zong, Akt and c-Myc differentially activate cellular metabolic programs and prime cells to bioenergetic inhibition, J. Biol. Chem. 285 (10) (2010) 7324–7333.
[26] S. Hu, et al., ^{13}C-Pyruvate imaging reveals alterations in glycolysis that precede c-Myc-induced tumor formation and regression, Cell Metabol. 14 (1) (2011) 131–142.
[27] F. Cui, et al., The involvement of c-Myc in the DNA double-strand break repair via regulating radiation-induced phosphorylation of ATM and DNA-PKcs activity, Mol. Cell. Biochem. 406 (1) (2015) 43–51.
[28] L.R. Edmunds, et al., c-Myc and AMPK control cellular energy levels by cooperatively regulating mitochondrial structure and function, PloS One 10 (7) (2015) e0134049.
[29] E.S. Goetzman, E.V. Prochownik, The role for Myc in coordinating glycolysis, oxidative phosphorylation, glutaminolysis, and fatty acid metabolism in normal and neoplastic tissues, Front. Endocrinol. 9 (2018) 129-129.
[30] L. Yu, et al., Modeling the genetic regulation of cancer metabolism: interplay between glycolysis and oxidative phosphorylation, Canc. Res. 77 (7) (2017) 1564–1574.
[31] D. Jia, et al., Elucidating the metabolic plasticity of cancer: mitochondrial reprogramming and hybrid metabolic States, Cells 7 (3) (2018) 21.
[32] D. Jia, et al., Elucidating cancer metabolic plasticity by coupling gene regulation with metabolic pathways, Proc. Natl. Acad. Sci. Unit. States Am. 116 (9) (2019) 3909.
[33] Y. Xu, et al., Structure of the protein phosphatase 2A holoenzyme, Cell 127 (6) (2006) 1239–1251.
[34] U.S. Cho, W. Xu, Crystal structure of a protein phosphatase 2A heterotrimeric holoenzyme, Nature 445 (7123) (2007) 53–57.
[35] F. Li, et al., Myc stimulates nuclearly encoded mitochondrial genes and mitochondrial biogenesis, Mol. Cell Biol. 25 (14) (2005) 6225.
[36] F. Morrish, et al., The oncogene c-Myc coordinates regulation of metabolic networks to enable rapid cell cycle entry, Cell Cycle 7 (8) (2008) 1054–1066.
[37] J.A. Graves, et al., Regulation of reactive oxygen species homeostasis by peroxiredoxins and c-myc, J. Biol. Chem. 284 (10) (2009) 6520–6529.
[38] K.-m. Lee, et al., MYC and MCL1 cooperatively promote chemotherapy-resistant breast cancer stem cells via regulation of mitochondrial oxidative phosphorylation, Cell Metabol. 26 (4) (2017) 633–647 e7.
[39] C.Y. Huang, et al., SOD1 down-regulates NF-kappaB and c-Myc expression in mice

after transient focal cerebral ischemia, J. Cerebr. Blood Flow Metabol. 21 (2) (2001) 163–173.
[40] P. Joseph, et al., Cadmium-induced cell transformation and tumorigenesis are associated with transcriptional activation of c-fos, c-jun, and c-Myc proto-oncogenes: role of cellular calcium and reactive oxygen species, Toxicol. Sci. 61 (2) (2001) 295–303.
[41] M. Welcker, et al., The Fbw7 tumor suppressor regulates glycogen synthase kinase 3 phosphorylation-dependent c-Myc protein degradation, Proc. Natl. Acad. Sci. U. S. A. 101 (24) (2004) 9085–9090.
[42] M. Yada, et al., Phosphorylation-dependent degradation of c-Myc is mediated by the F-box protein Fbw7, EMBO J. 23 (10) (2004) 2116–2125.
[43] K. Noguchi, et al., Regulation of c-Myc through phosphorylation at ser-62 and ser-71 by c-jun N-terminal kinase, J. Biol. Chem. 274 (46) (1999) 32580–32587.
[44] J.R. Escamilla-Powers, R.C. Sears, A conserved pathway that controls c-Myc protein stability through opposing phosphorylation events occurs in yeast, J. Biol. Chem. 282 (8) (2007) 5432–5442.
[45] B. McCright, D.M. Virshup, Identification of a new family of protein phosphatase 2A regulatory subunits, J. Biol. Chem. 270 (44) (1995) 26123–26128.
[46] P. Seshacharyulu, et al., Phosphatase: PP2A structural importance, regulation and its aberrant expression in cancer, Canc. Lett. 335 (1) (2013) 9–18.
[47] M. Suganuma, et al., Okadaic acid: an additional non-phorbol-12-tetradecanoate-13-acetate-type tumor promoter, Proc. Natl. Acad. Sci. U.S.A. 85 (6) (1988) 1768–1771.
[48] D.C. Pallas, et al., Polyoma small and middle T antigens and SV40 small t antigen form stable complexes with protein phosphatase 2A, Cell 60 (1) (1990) 167–176.
[49] S.S. Wang, et al., Alterations of the PPP2R1B gene in human lung and colon cancer, Science 282 (5387) (1998) 284–287.
[50] A.S. Farrell, et al., Targeting inhibitors of the tumor suppressor PP2A for the treatment of pancreatic cancer, Mol. Canc. Res. : MCR 12 (6) (2014) 924–939.
[51] E. Wandzioch, et al., PME-1 modulates protein phosphatase 2A activity to promote the malignant phenotype of endometrial cancer cells, Canc. Res. 74 (16) (2014) 4295–4305.
[52] H. Liu, et al., Overexpression of PP2A inhibitor SET oncoprotein is associated with tumor progression and poor prognosis in human non-small cell lung cancer, Oncotarget 6 (17) (2015) 14913–14925.
[53] M. Mumby, PP2A: unveiling a reluctant tumor suppressor, Cell 130 (1) (2007) 21–24.
[54] I.C. Low, et al., Ser70 phosphorylation of Bcl-2 by selective tyrosine nitration of PP2A-B56delta stabilizes its antiapoptotic activity, Blood 124 (14) (2014) 2223–2234.
[55] B. Ahn, H. Ohshima, Suppression of intestinal polyposis in **Apc$^{Min/+}$** mice by inhibiting nitric oxide production, Canc. Res. 61 (23) (2001) 8357–8360.
[56] L.R. Kisley, et al., Genetic ablation of inducible nitric oxide synthase decreases mouse lung tumorigenesis, Canc. Res. 62 (23) (2002) 6850–6856.
[57] J. Sangodkar, et al., Activation of tumor suppressor protein PP2A inhibits KRAS-driven tumor growth, J. Clin. Invest. 127 (6) (2017) 2081–2090.
[58] M. Niyazi, I. Niyazi, C. Belka, Counting colonies of clonogenic assays by using densitometric software, Radiat. Oncol. 2 (2007) 4-4.